

# Electrochemical and Spectroelectrochemical Studies on $\text{UO}_2(\text{saloph})\text{L}$ (saloph = *N,N*-Disalicylidene-*o*-phenylenediaminate, L = Dimethyl Sulfoxide or *N,N*-Dimethylformamide)

Koichiro Mizuoka,<sup>†</sup> Seong-Yun Kim,<sup>†</sup> Miki Hasegawa,<sup>§</sup> Toshihiko Hoshi,<sup>§</sup> Gunzo Uchiyama,<sup>†</sup> and Yasuhisa Ikeda<sup>\*†</sup>

Research Laboratory for Nuclear Reactors, Tokyo Institute of Technology, O-okayama, Meguro-ku, Tokyo 152-8550, Japan, Japan Atomic Energy Research Institute, Tokai, Ibaraki 319-1195, Japan, and Department of Chemistry, College of Science and Engineering, Aoyama Gakuin University, Chitosedai, Setagaya-ku, Tokyo 157-8572, Japan

Received October 8, 2002

To examine properties of pentavalent uranium, U(V), we have carried out electrochemical and spectroelectrochemical studies on  $\text{UO}_2(\text{saloph})\text{L}$  [saloph = *N,N*-disalicylidene-*o*-phenylenediaminate, L = dimethyl sulfoxide (DMSO) or *N,N*-dimethylformamide (DMF)]. The electrochemical reactions of  $\text{UO}_2(\text{saloph})\text{L}$  complexes in L were found to occur quasireversibly. The reduction processes of  $\text{UO}_2(\text{saloph})\text{L}$  complexes were followed spectroelectrochemically by using an optical transparent thin layer electrode cell. It was found that the absorption spectra measured at the applied potentials from 0 to  $-1.650$  V versus ferrocene/ferrocenium ion redox couple (Fc/Fc<sup>+</sup>) for  $\text{UO}_2(\text{saloph})\text{-DMSO}$  in DMSO have clear isosbestic points and that the evaluated electron stoichiometry equals 1.08. These results indicate that the reduction product of  $\text{UO}_2(\text{saloph})\text{DMSO}$  is  $[\text{U}^{\text{V}}\text{O}_2(\text{saloph})\text{DMSO}]^-$ , which is considerably stable in DMSO. Furthermore, it was clarified that the absorption spectrum of the  $[\text{U}^{\text{V}}\text{O}_2(\text{saloph})\text{DMSO}]^-$  complex has a very small molar absorptivity in the visible region and characteristic absorption bands due to the 5f<sup>1</sup> orbital at around 750 and 900 nm. For  $\text{UO}_2(\text{saloph})\text{DMF}$  in DMF, the clear isosbestic points were not observed in the similar spectral changes. It is proposed that the  $\text{UO}_2(\text{saloph})\text{DMF}$  complex is reduced to  $[\text{U}^{\text{V}}\text{O}_2(\text{saloph})\text{DMF}]^-$  accompanied by the dissociation of DMF as a successive reaction. The formal redox potentials of  $\text{UO}_2(\text{saloph})\text{L}$  in L ( $E^0$ , vs Fc/Fc<sup>+</sup>) for U(VI)/U(V) couple were determined to be  $-1.550$  V for L = DMSO and  $-1.626$  V for L = DMF.

## 1. Introduction

Uranium has various oxidation states, III, IV, V, and VI in solution. In these oxidation states, pentavalent uranium, U(V), is the most unstable species, because of its disproportionation,<sup>1</sup> that is  $2\text{U}^{\text{V}}\text{O}_2^+ \rightarrow \text{U}^{\text{IV}}\text{O}_2 + \text{U}^{\text{VI}}\text{O}_2^{2+}$ . Therefore, properties of U(V) have not been understood sufficiently.

Studies on the properties of U(V) have been carried out by electrochemical and photochemical reduction of U(VI)

species.<sup>2–14</sup> Previously, we have also investigated the electrochemical properties of  $[\text{UO}_2(\text{CO}_3)]^{4-}$  in aqueous solu-

\* To whom correspondence should be addressed. E-mail: yiked@nr.titech.ac.jp. Phone and fax: +81-3-5734-3061.

<sup>†</sup> Tokyo Institute of Technology.

<sup>§</sup> Japan Atomic Energy Research Institute.

<sup>§</sup> Aoyama Gakuin University.

(1) (a) Heal, H. G. *Trans. Faraday Soc.* **1949**, *45*, 1–11. (b) Heal, H. G.; Thomas, J. G. N. *Trans. Faraday Soc.* **1949**, *45*, 11–20. (c) Newton, T. W.; Baker, F. B. *Inorg. Chem.* **1965**, *4*, 1166–1170. (d) Ekstrom, A. *Inorg. Chem.* **1974**, *13*, 2237–2241.

(2) (a) Selbin, J.; Ortego, J. D. *Chem. Rev.* **1969**, *69*, 657–671. (b) Sipos, L.; Jeftić, L. J.; Branica, M. *Electroanal. Chem.* **1971**, *32*, 35–47. (c) Halstead, G. W.; Eller, P. G.; Eastman, M. P. *Inorg. Chem.* **1979**, *18*, 2867–2872. (d) Folcher, G.; Lambard, J.; de Villardi, G. C. *Inorg. Chim. Acta* **1980**, *45*, L59–L61. (e) Zanello, P.; Cinquantini, A.; Mazzocchin, G. A. *J. Electroanal. Chem.*, **1982**, *131*, 215–27. (f) Eller, P. G.; Vergamini, P. J. *Inorg. Chem.* **1983**, *22*, 3184–3189. (g) Seeber, R.; Zanello, P. *J. Chem. Soc., Dalton Trans.* **1985**, 601–603. (h) Harazono, T.; Fukutomi, H. *Bull. Chem. Soc. Jpn.* **1986**, *59*, 2129–2133. (i) Hitchcock, P. B.; Mohammed, T. J.; Seddon, K. R.; Zora, J. A. *Inorg. Chim. Acta* **1986**, *113*, L25–L26. (j) Howes, K. R.; Bakac, A.; Espenson, J. H. *Inorg. Chem.* **1988**, *27*, 791–94. (k) Sandhu, S. S.; Singh, R. J.; Chawla, S. K. *J. Photochem. Photobiol., A* **1990**, *52*, 65–68. (l) Bakac, A.; Espenson, J. H. *Inorg. Chem.* **1995**, *34*, 1730–1735.

(3) Mizuguchi, K.; Park, Y.-Y.; Tomiyasu, H.; Ikeda, Y. *J. Nucl. Sci. Technol.* **1993**, *30*, 542–548. From this paper, the  $\epsilon$  values of  $[\text{U}^{\text{VI}}\text{O}_2(\text{CO}_3)_3]^{4-}$  and its U(V) species at 448 nm are found to be 24 and 5 M<sup>-1</sup>cm<sup>-1</sup>, respectively.

tions<sup>3</sup>, and  $[\text{UO}_2(\text{L})_5]^{2+}$  (L = dimethyl sulfoxide, DMSO or *N,N*-dimethylformamide, DMF),  $\text{UO}_2(\beta\text{-diketonato})_2\text{L}$  ( $\beta$ -diketonate = acetylacetonate, dibenzoylmethanate, trifluoroacetylacetonate, and hexafluoroacetylacetonate), and  $\text{UO}_2(\text{salen})\text{DMF}$  (salen = *N,N'*-disalicylideneethylenediamine) in nonaqueous solutions.<sup>5–7</sup> From these studies, we proposed that these uranyl complexes are reduced reversibly or quasireversibly to form relatively stable U(V) species, that the resulting U(V) species are presumably yl-type,  $\text{U}^{\text{V}}\text{O}_2^+$ , and that uranyl complexes with multidentate ligand(s) can form more stable U(V) complexes than those with unidentate ligands,  $[\text{UO}_2(\text{L})_5]^{2+}$ .

Furthermore, many researchers have investigated the spectroscopic properties of U(V) species in aqueous<sup>8,9</sup> and in nonaqueous solvents.<sup>10–14</sup> They reported that the U(V) species has characteristic absorption bands in visible and near-infrared regions, that is, 765 and 980 nm in  $\text{K}_2\text{CO}_3$  aqueous solution, and 750, 950, and 1500 nm in nonaqueous solvent. However, in most of previous reports, sample solutions were mixtures of U(IV), U(V), and U(VI) species, and the absorption bands of U(V) were assigned by comparing them with those of U(IV) and U(VI) species. Therefore, their assignments are still uncertain.

On the other hand, we carried out spectroelectrochemical measurements on  $[\text{UO}_2(\text{CO}_3)_3]^{4-}$  with an optical transparent thin layer electrode (OTTLE) cell<sup>15</sup> in  $\text{Na}_2\text{CO}_3$  aqueous solution.<sup>3</sup> In this study, we succeeded in determining the electron stoichiometry to be 1 and in obtaining the first clear electronic spectrum of pure U(V) carbonate complex in aqueous system. As a result, we proposed that the U(V) carbonate complex has a very small molar absorptivity ( $\epsilon$ ) in the visible region; that is, the  $\epsilon$  value is  $5 \text{ M}^{-1}\cdot\text{cm}^{-1}$  ( $\text{M} = \text{mol}\cdot\text{dm}^{-3}$ ) at 448 nm. However, we could not confirm whether the characteristic absorption bands of U(V) species exist at around 765, 980, and 1500 nm.

To confirm the validity of our proposal, hence, we investigated the electrochemical and spectroelectrochemical properties of uranyl complexes with *N,N'*-disalicylidene-*o*-phenylenediamine (saloph<sup>2-</sup>) as tetradentate ligand and DMSO or DMF as unidentate ligand, that is,  $\text{UO}_2(\text{saloph})\text{-DMSO}$  and  $\text{UO}_2(\text{saloph})\text{DMF}$  (see Figure 1).

## 2. Experimental Section

**Materials.** *N,N'*-Disalicylidene-*o*-phenylenediamine ( $\text{H}_2\text{saloph}$ , see Figure 1) was synthesized according to the procedure reported in the previous paper<sup>16</sup> and purified by recrystallization from ethyl

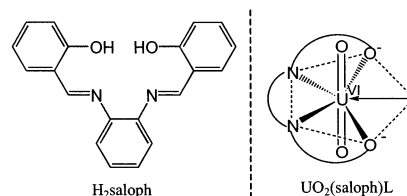


**Figure 1.** Schematic structures of  $\text{H}_2\text{saloph}$  and  $\text{UO}_2(\text{saloph})\text{L}$  complexes, L = DMSO or DMF.

acetate. Ethanol solution of  $\text{UO}_2(\text{NO}_3)_2\cdot n\text{H}_2\text{O}$  (2.0 g) was added dropwise to hot ethanol solution containing  $\text{H}_2\text{saloph}$  (1.3 g, 4.1 mmol) under vigorous stirring. The mixture was refluxed for 2 h at 78 °C. Then, the mixture was cooled at  $-18$  °C for 1 week. The precipitate of  $\text{UO}_2(\text{saloph})\text{EtOH}$  was filtrated and washed with ethanol. The  $\text{UO}_2(\text{saloph})\text{EtOH}$  (0.3 g, 0.48 mmol) was dissolved in DMSO or DMF. The solutions were heated at 80 °C with stirring for 3 h and kept at 100 °C for 48 h under vacuum to remove solvents. The  $\text{UO}_2(\text{saloph})\text{L}$  (L = DMSO or DMF) complexes were precipitated as orange needle crystals and recrystallized from dichloromethane and ether.

Dimethyl sulfoxide (Kanto Chemical Co., Ind.), DMF (Kanto), and dichloromethane (Kanto) were dried over molecular sieves 4A (Wako Pure Chemical Ind., Ltd.) before electrochemical measurements. Tetra-*n*-butylammonium perchlorate (TBAP, Fluka, electrochemical grade) as supporting electrolyte was used as received without further purification. All other chemicals used were of reagent grade.

Anal. Calcd for  $\text{UO}_2(\text{saloph})\text{DMSO}$ : C, 39.88; H, 3.04; N, 4.23; S, 4.84. Found: C, 39.89; H, 3.02; N, 4.38; S, 4.20. <sup>1</sup>H NMR ( $\delta$ /ppm, in dichloromethane-*d*<sub>2</sub>, relative to TMS): 3.07 (s, 6H, methyl group of DMSO), 6.74–7.90 (m, 12H, phenyl group), 9.38 (s, 2H, azomethine group). IR ( $\text{cm}^{-1}$ , in KBr powder); 1605 ( $\nu_{\text{C-N}}$ ), 999 ( $\nu_{\text{S-O}}$ ), 897 ( $\nu_{\text{U-O}}$ ).

Anal. Calcd for  $\text{UO}_2(\text{saloph})\text{DMF}$ : C, 42.02; H, 3.22; N, 6.39. Found: C, 42.08; H, 3.37; N, 6.52. <sup>1</sup>H NMR ( $\delta$ /ppm, in dichloromethane-*d*<sub>2</sub>, relative to TMS): 3.11 (s, 6H, methyl group of DMF), 6.79–7.89 (m, 12H, phenyl group), 8.52 (vs, 1H, formyl group of DMF), 9.39 (s, 2H, azomethine group). IR ( $\text{cm}^{-1}$ , in KBr powder); 1651 ( $\nu_{\text{C-O}}$ ), 1609 ( $\nu_{\text{C-N}}$ ), 905 ( $\nu_{\text{U-O}}$ ).

**Methods.** We used cyclic voltammetry (CV) for electrochemical studies. The CV measurements were carried out at 25 °C under dry argon atmosphere using BAS CV-50W voltammetric analyzer and BAS CV cell. A three-electrode system was utilized, that is, a BAS 002013 as Pt working electrode (electrode surface area 0.020  $\text{cm}^2$ ), a BAS 002222 as Pt counter electrode, and a BAS 002025 RE-5 as Ag/Ag<sup>+</sup> reference electrode. A ferrocene/ferrocenium ion redox couple ( $\text{Fc}/\text{Fc}^+$ ) was used as the standard redox system in the present study as recommended by IUPAC.<sup>17</sup> The formal potentials of  $\text{Fc}/\text{Fc}^+$  were 0.073 V in DMSO and 0.119 V in DMF versus Ag/Ag<sup>+</sup> reference electrode, respectively. All potentials reported here are versus  $\text{Fc}/\text{Fc}^+$ . All sample solutions were deoxygenated by passing argon gas into the solutions for at least 10 min prior to starting the CV measurements.

Spectroelectrochemical studies were performed using Agilent 8453 diode-array spectrophotometer equipped with an OTTLE

- (4) Mizuguchi, K. Ph.D. thesis, Tokyo Institute of Technology, 1999.
- (5) Kim, S.-Y.; Tomiyasu, H.; Ikeda, Y. *J. Nucl. Sci. Technol.* **2002**, *39*, 160–165.
- (6) Lee, S.-H.; Mizuguchi, K.; Tomiyasu, H.; Ikeda, Y. *J. Nucl. Sci. Technol.* **1996**, *33*, 190–192.
- (7) Mizuguchi, K.; Lee, S.-H.; Ikeda, Y.; Tomiyasu, H. *J. Alloys Compd.* **1998**, *271–272*, 163–167.
- (8) Cohen, D. *J. Inorg. Nucl. Chem.* **1970**, *32*, 3525–3530.
- (9) Bell, J. T.; Friedman, H. A.; Billings, M. R. *J. Inorg. Nucl. Chem.* **1974**, *36*, 2563–2567.
- (10) Gritzner, G.; Selbin, J. *J. Inorg. Nucl. Chem.* **1968**, *30*, 1799–1804.
- (11) Miyake, C.; Yamana, Y.; Imoto, S. *Inorg. Chim. Acta* **1984**, *95*, 17–21.
- (12) Fukutomi, H.; Harazono, T. *Bull. Chem. Soc. Jpn.* **1986**, *59*, 3678–3680.
- (13) Miyake, C.; Kondo, T.; Imoto, S. *J. Less-Common Met.* **1986**, *122*, 313–317.

- (14) Monjushiro, H.; Hara, H.; Yokoyama, Y. *Polyhedron* **1992**, *11*, 845–846.
- (15) Heineman, W. R. *J. Chem. Educ.* **1983**, *60*, 305–308.
- (16) Pfeiffer, P.; Hesse, T.; Pfitzinger, H.; Scholl, W.; Thielert, H. *J. Prakt. Chem.* **1937**, *149*, 217–296.
- (17) Gritzner, G.; Kůta, J. *Pure Appl. Chem.* **1984**, *56*, 461–466.

cell,<sup>15,18</sup> which has Pt minigrad electrode as optical transparent working electrode. The optical path length was ca. 0.03 cm and calibrated spectrophotometrically for every measurement ( $2.90 \times 10^{-2}$  cm for  $\text{UO}_2(\text{saloph})\text{DMSO}$  in DMSO,  $2.76 \times 10^{-2}$  cm for  $\text{UO}_2(\text{saloph})\text{DMF}$  in DMF). Other conditions for spectroelectrochemical measurements were same as those of CV measurements. The electronic spectral changes during electrochemical reaction were observed with spectropotentiostatic technique, in which the spectrum at each applied potential was measured after equilibrium was achieved. In the present experiments, the equilibrium was evidenced by cessation of absorbance changes and required at least 2 min.

Characterizations of the uranyl complexes were performed with NMR spectrophotometer (JEOL JNM-LA300WB, 300.4 MHz), IR spectrophotometer (Shimadzu FTIR-8100), and elemental analyzer (Thermo Finnigan Flash EA1112 CHNS-O elemental analyzer).

### 3. Results and Discussion

**3.1.  $\text{UO}_2(\text{saloph})\text{DMSO}$  in DMSO.** Cyclic voltammograms of  $\text{UO}_2(\text{saloph})\text{DMSO}$  ( $9.55 \times 10^{-4}$  M) in DMSO containing TBAP (0.10 M) are shown in Figure 2. Peaks ( $P_{\text{cs}}$  and  $P_{\text{as}}$ ) of one redox couple are observed at around  $-1.60$  ( $E_{\text{pcs}}$ ) and  $-1.50$  V ( $E_{\text{pas}}$ ). The electrochemical data are collected in Table 1. Peak potential separations ( $\Delta E_{\text{p}} = E_{\text{pcs}} - E_{\text{pas}}$ ) increase from 0.093 to 0.108 V with an increase in scan rate ( $\nu$ ). Formal potential [ $E_{\text{s}}^0 = (E_{\text{pas}} - E_{\text{pcs}})/2$ ] is constant,  $-1.550 \pm 0.002$  V (or  $-0.917$  V vs SHE), without depending on  $\nu$ . Ratios of peak currents ( $i_{\text{pas}}/i_{\text{pcs}}$ ) were calculated from the semiempirical equation, eq 1:<sup>19</sup>

$$i_{\text{pa}}/i_{\text{pc}} = i_{\text{pa0}}/i_{\text{pc0}} + (0.485 \times i_{\text{sp0}})/i_{\text{pc0}} + 0.086 \quad (1)$$

where  $i_{\text{pa0}}$ ,  $i_{\text{pc0}}$ , and  $i_{\text{sp0}}$  are currents measured with respect to the zero current axis at anodic peak potential, cathodic peak potential, and switching potential, respectively. The  $i_{\text{pas}}/i_{\text{pcs}}$  values are almost 1 without depending on  $\nu$  (see Table 1). From these results, it is suggested that the electrochemical reaction is a quasireversible system and has no successive reactions to produce electrochemically active substances.

For a more detailed discussion of the electrochemical reaction mechanism in this system, the spectroelectrochemical measurements were carried out for the DMSO solution containing  $\text{UO}_2(\text{saloph})\text{DMSO}$  ( $8.56 \times 10^{-4}$  M) and TBAP (0.30 M). Electronic spectra were measured at the applied potentials in the range from 0 to  $-1.650$  V. The results are shown in Figure 3. Clear isosbestic points are observed at 271, 387, 479, and 535 nm in Figure 3a,b. This indicates that one equilibrium exists in this system. The redox equilibrium of  $\text{UO}_2(\text{saloph})\text{DMSO}$  at  $E_{\text{pcs}}/E_{\text{pas}}$  is proposed as the most probable candidate.

To determine the electron stoichiometry ( $n$  value) for this redox couple, the Nernstian plot is performed for the absorbancies at 344 nm in Figure 3 and is shown in Figure 4. From the intercept and reciprocal slope of this plot, the values of  $E_{\text{s}}^0$  and  $n$  were calculated as  $-1.550$  V and 1.08 at 25 °C, respectively. Hence, it is concluded that the redox couple at  $E_{\text{pcs}}/E_{\text{pas}}$  corresponds to the following reaction:

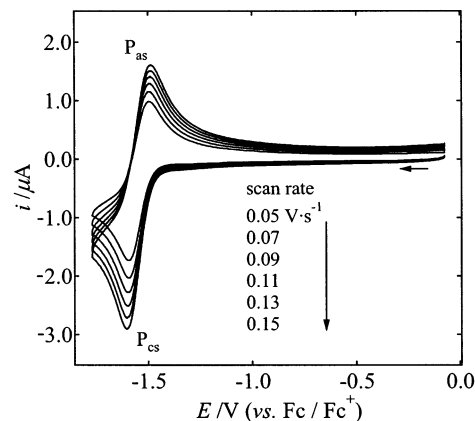
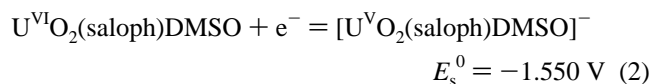


**Figure 2.** Cyclic voltammograms of  $\text{UO}_2(\text{saloph})\text{DMSO}$  ( $9.55 \times 10^{-4}$  M) in DMSO containing 0.10 M TBAP measured in the potential range from  $-0.073$  to  $-1.773$  V at different scan rates ( $\nu = 0.05$ – $0.15$   $\text{V}\cdot\text{s}^{-1}$ ). Initial scan direction: cathodic.

**Table 1.** Electrochemical Data for  $\text{UO}_2(\text{saloph})\text{DMSO}$  in DMSO

$\nu/\text{V}\cdot\text{s}^{-1}$	$E_{\text{pcs}}/\text{V}$	$E_{\text{pas}}/\text{V}$	$i_{\text{pcs}}/\mu\text{A}$	$i_{\text{pas}}/i_{\text{pcs}}$
0.05	-1.594	-1.501	1.596	0.97
0.07	-1.593	-1.502	1.857	0.99
0.09	-1.597	-1.501	2.092	0.99
0.11	-1.600	-1.498	2.295	1.00
0.13	-1.604	-1.496	2.482	0.99
0.15	-1.606	-1.498	2.649	0.99

Furthermore, to evaluate the validity of assignment that the electrochemical reaction 2 is quasireversible, the standard rate constant ( $k^0$ ) was estimated by Nicholson's equation [eq 3]<sup>20,21</sup> on the basis of the assumption that diffusion coefficients of oxidant ( $D_{\text{O}}$ ) and reductant ( $D_{\text{R}}$ ) are equal:

$$\psi = k^0 / \{D_{\text{O}}\pi(nF/RT)v\}^{1/2} \quad (3)$$

where  $\psi$  is the kinetic parameter defined by Nicholson.<sup>20</sup> The  $D_{\text{O}}$  value was estimated by eq 4:<sup>21</sup>

$$i_{\text{pc}} = 2.985 \times 10^2 n A C_{\text{O}}^0 (\alpha n_{\text{B}})^{1/2} v^{1/2} D_{\text{O}}^{1/2} \quad (4)$$

In eq 4,  $A$ ,  $C_{\text{O}}^0$ ,  $\alpha$ , and  $n_{\text{B}}$  are surface area of working electrode, concentration of oxidant, transfer coefficient, and electron stoichiometry in rate-determining process, respectively. The  $\alpha n_{\text{B}}$  value was obtained as 0.72 from eq 5:<sup>22</sup>

$$\alpha n_{\text{B}} = 0.04768 / (E_{\text{p}2} - E_{\text{p}}) \quad (5)$$

where  $E_{\text{p}}$  and  $E_{\text{p}2}$  are peak potential and half peak potential, respectively. Hence, the  $D_{\text{O}}$  value was estimated as  $2.1 \times 10^{-6}$   $\text{cm}^2\cdot\text{s}^{-1}$  by eq 4. The  $\psi$  values are in the range from 0.70 ( $\nu = 0.05$   $\text{V}\cdot\text{s}^{-1}$ ,  $\Delta E_{\text{p}} = 0.093$  V) to 0.46 ( $\nu = 0.15$   $\text{V}\cdot\text{s}^{-1}$ ,  $\Delta E_{\text{p}} = 0.108$  V).<sup>20,21</sup> Thus, the  $k^0$  value of the electrochemical reaction 2 is estimated as  $2.9 \times 10^{-3}$   $\text{cm}\cdot\text{s}^{-1}$  by using eq 3.

(18) Endo, A.; Mochida, I.; Shimizu, K.; Satō, G. *P. Anal. Sci.* **1995**, *11*, 457–459.

(19) Nicholson, R. S. *Anal. Chem.* **1966**, *38*, 1406.

(20) Nicholson, R. S. *Anal. Chem.* **1965**, *37*, 1351–1355.

(21) Heinze, J. *Angew. Chem., Int. Ed. Engl.* **1984**, *23*, 831–847.

(22) Nicholson, R. S.; Shain, I. *Anal. Chem.* **1964**, *36*, 706–723.

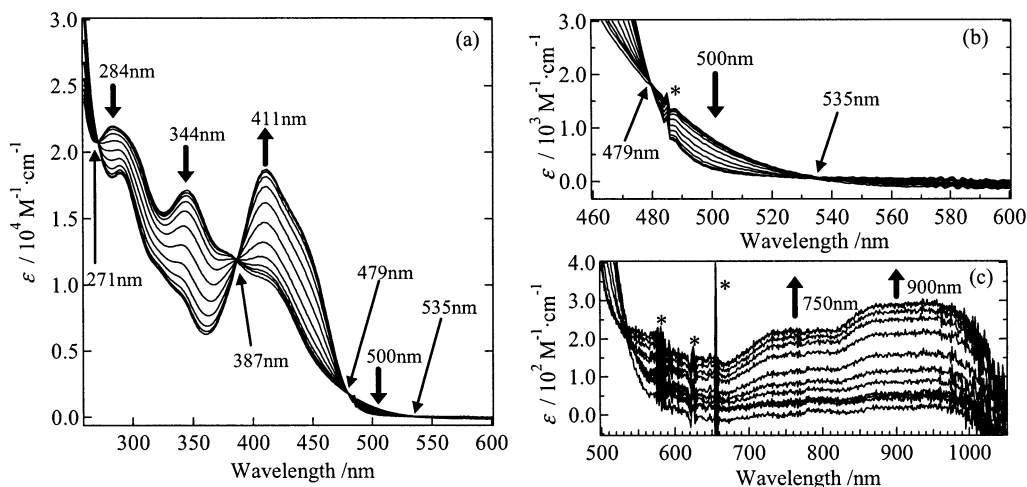


**Figure 3.** Electronic spectra measured at the applied potentials in the range from 0 to  $-1.650$  V for  $\text{UO}_2(\text{saloph})\text{DMSO}$  ( $8.56 \times 10^{-4}$  M) in DMSO solution containing  $0.30$  M TBAP. Wavelength range: (a) 260–600, (b) 460–600, and (c) 500–1050 nm. Asterisk indicates noise of equipment.

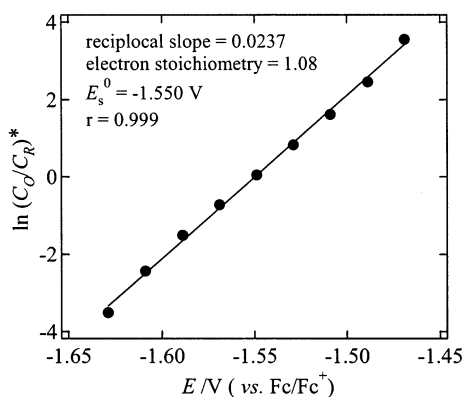


**Figure 4.** Nernstian plot for the absorbancies at 344 nm in Figure 3. Asterisk indicates natural logarithm of concentration ratio of oxidant ( $C_O$ ) to reductant ( $C_R$ ).

Matsuda et al. have proposed reversibility factor ( $\Lambda$ ) for electrochemical reactions.<sup>23</sup> The  $\Lambda$  value is defined by eq 6 for  $D_O = D_R$ :

$$\Lambda = k^0 / (D_O n F v / RT)^{1/2} \quad (6)$$

For a reversible system,  $\Lambda > 15$ , for a quasireversible system,  $15 > \Lambda > 10^{-2(1+\alpha)}$ , and for an irreversible system,  $10^{-2(1+\alpha)} > \Lambda$ .

If the relation  $D_O = D_R = 2.1 \times 10^{-6} \text{ cm}^2 \cdot \text{s}^{-1}$  holds in the electrochemical reaction 2, the equation of  $\Lambda$  is expressed as  $1.1 \times 10^2 k^0 / v^{1/2}$ . In  $\alpha = 0.72$  ( $n_B = 1$ ), the following relationships for the  $k^0$  value are derived in the range  $v = 0.05$ – $0.15 \text{ V} \cdot \text{s}^{-1}$ .

For a reversible system,  $k^0 > (3.0\text{--}5.3) \times 10^{-2}$ , for a quasireversible system,  $(3.0\text{--}5.3) \times 10^{-2} > k^0 > (0.73\text{--}1.3) \times 10^{-6}$ , and for an irreversible system,  $(0.73\text{--}1.3) \times 10^{-6} > k^0$ .

These classifications support that the electrochemical reaction 2 is quasireversible under the present experimental conditions, because the estimated  $k^0$  value ( $= 2.9 \times 10^{-3} \text{ cm} \cdot \text{s}^{-1}$ ) is compatible with the range  $(3.0\text{--}5.3) \times 10^{-2} > k^0 > (0.73\text{--}1.3) \times 10^{-6}$ .

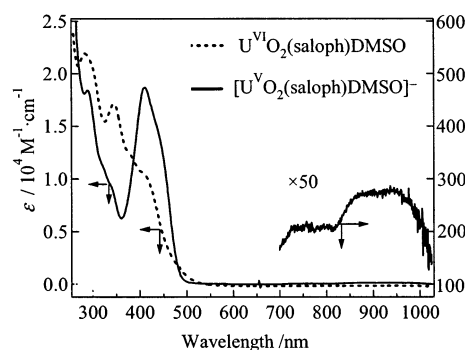


**Figure 5.** Electronic spectra of  $\text{U}^{\text{VI}}\text{O}_2(\text{saloph})\text{DMSO}$  (---) and  $[\text{U}^{\text{V}}\text{O}_2(\text{saloph})\text{DMSO}]^-$  (—) in DMSO.

As a result, it is concluded that the electrochemical reduction of  $\text{UO}_2(\text{saloph})\text{DMSO}$  in DMSO produces the very stable  $[\text{U}^{\text{V}}\text{O}_2(\text{saloph})\text{DMSO}]^-$  complex quasireversibly.

On the basis of these considerations, the spectrum obtained at  $-1.650$  V in Figure 3 is assigned to be  $[\text{U}^{\text{V}}\text{O}_2(\text{saloph})\text{DMSO}]^-$ . This is the electronic spectrum of the pure U(V) complex first observed in nonaqueous solvents. Previously, we reported that the  $\epsilon$  value of the absorption band due to uranyl ion in the visible region (at around 400–500 nm) decreases with the reduction from  $[\text{U}^{\text{VI}}\text{O}_2(\text{CO}_3)_3]^{4-}$  to U(V); that is, the aqueous solution containing  $\text{U}^{\text{V}}\text{O}_2^{2+}$  is almost colorless.<sup>3</sup> In the present study, the decrease of the  $\epsilon$  value at around 500 nm is clearly observed as shown in Figure 3b. This indicates that the disappearance of the absorption band at around 500 nm is characteristics of U(V) species in both aqueous and nonaqueous solvents. However, the “colorless” solution is not produced in the present system. This is considered to be due to spread of the large absorption bands of LM/MLCT and/or saloph<sup>2-</sup> ligand in this region.

Many researchers have proposed that the U(V) species have characteristic absorption bands due to the  $5f^1$  orbital at around 750 and 900 nm.<sup>8–14</sup> However, their proposal was not based on the observation of absorption spectra of pure U(V) species. We observed the appearance of the absorption bands at around 750 and 900 nm with the reduction from  $\text{U}^{\text{VI}}\text{O}_2(\text{saloph})\text{DMSO}$  to  $[\text{U}^{\text{V}}\text{O}_2(\text{saloph})\text{DMSO}]^-$  as shown in Figure 3c. The electronic spectra of  $\text{U}^{\text{VI}}\text{O}_2(\text{saloph})\text{DMSO}$

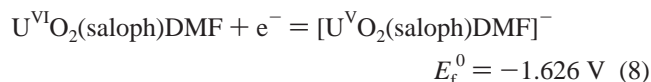
(23) Matsuda, H.; Ayabe, Y. *Z. Elektrochem.* **1955**, *59*, 494–503.

and  $[\text{U}^{\text{V}}\text{O}_2(\text{saloph})\text{DMSO}]^-$  are displayed in Figure 5 for comparison with each other. It is concluded from this figure that the absorption bands at around 750 and 900 nm are characteristics of  $\text{U}(\text{V})$  complexes.

**3.2.  $\text{UO}_2(\text{saloph})\text{DMF}$  in DMF.** Cyclic voltammograms of  $\text{UO}_2(\text{saloph})\text{DMF}$  ( $8.71 \times 10^{-4}$  M) in DMF containing TBAP (0.10 M) are shown in Figure 6. Peaks ( $P_{\text{cf}1}$  and  $P_{\text{af}1}$ ) of one redox couple and an uncoupled oxidation peak ( $P_{\text{af}2}$ ) are observed at around  $-1.69$  ( $E_{\text{pcf}1}$ ),  $-1.56$  ( $E_{\text{paf}1}$ ), and  $-1.00$  V ( $E_{\text{paf}2}$ ), respectively. The electrochemical data from CV measurements are collected in Table 2. The  $\Delta E_p$  ( $=E_{\text{pcf}1} - E_{\text{paf}1}$ ) values are in the range from 0.101 to 0.168 V with an increase in  $\nu$ . The formal potential [ $E_f^0 = (E_{\text{paf}1} - E_{\text{pcf}1})/2$ ] is constant,  $-1.626 \pm 0.005$  V (or  $-0.947$  V vs SHE), without depending on  $\nu$ . The  $i_{\text{paf}1}/i_{\text{pcf}1}$  values calculated by eq 1 are smaller than 1 and increase with increasing  $\nu$ . From these results, it is suggested that the electrochemical reaction of  $\text{UO}_2(\text{saloph})\text{DMF}$  in DMF is a quasireversible system accompanied by successive reaction of reduction product.

The spectroelectrochemical measurements were carried out for the DMF solution containing  $\text{UO}_2(\text{saloph})\text{DMF}$  ( $9.33 \times 10^{-4}$  M) and TBAP (0.3 M) to examine the electrochemical reaction mechanism. The electronic spectra measured at the applied potentials in the range from 0 to  $-1.785$  V are shown in Figure 7. As seen from this figure, any clear isosbestic points are not observed. This indicates that the reduction of  $\text{U}^{\text{VI}}\text{O}_2(\text{saloph})\text{DMF}$  is followed by successive reactions.

The  $n$  value in this electrochemical reaction could not be calculated by the Nernstian plot, because of the lack of clear isosbestic points. However, the tendency in the spectral changes is very similar to that of  $\text{UO}_2(\text{saloph})\text{DMSO}$  in DMSO except for the appearance of the absorption band at 640 nm. Furthermore, to confirm whether the products of reduction and successive reactions are completely oxidized to  $\text{U}^{\text{VI}}\text{O}_2(\text{saloph})\text{DMF}$ , electronic spectra were measured at the potentials applied from  $-1.785$  to 0 V. The spectral changes are consistent with those in Figure 7. These phenomena verify that the  $\text{U}^{\text{VI}}\text{O}_2(\text{saloph})\text{DMF}$  complex is reduced to  $[\text{U}^{\text{V}}\text{O}_2(\text{saloph})\text{DMF}]^-$  with successive reactions and that the successive reaction is not the irreversible one such as the disproportionation [ $2\text{U}^{\text{V}}\text{O}_2 \rightarrow \text{U}^{\text{VI}}\text{O}_2 + \text{U}^{\text{VI}}\text{O}_2^{2+}$ ]. As the most probable successive reaction, the structural change of  $[\text{U}^{\text{V}}\text{O}_2(\text{saloph})\text{DMF}]^-$  can be proposed. Hence, the electrochemical reaction of  $\text{UO}_2(\text{saloph})\text{DMF}$  in DMF is considered to take place through the following EC mechanism:<sup>24</sup>



where  $[\text{U}(\text{V})_{\text{scc}}]$  is the product in the successive reaction and  $[\text{U}(\text{VI})_{\text{scc}}]$  is the oxidation product of  $[\text{U}(\text{V})_{\text{scc}}]$  at  $E_{\text{paf}2}$ .

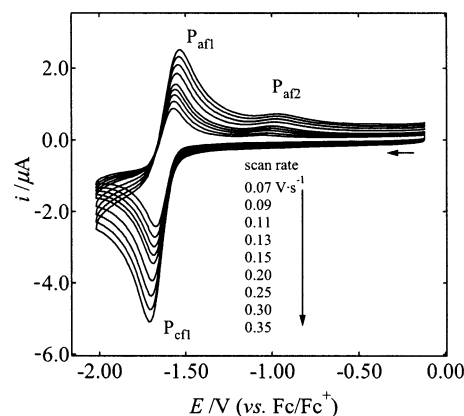


**Figure 6.** Cyclic voltammograms of  $\text{UO}_2(\text{saloph})\text{DMF}$  ( $8.71 \times 10^{-4}$  M) in DMF containing 0.10 M TBAP measured in the potential range from  $-0.119$  to  $-2.019$  V at different scan rates ( $\nu = 0.07$ – $0.35$   $\text{V}\cdot\text{s}^{-1}$ ). Initial scan direction: cathodic.

**Table 2.** Electrochemical Data for  $\text{UO}_2(\text{saloph})\text{DMF}$  in DMF

$\nu / \text{V}\cdot\text{s}^{-1}$	$E_{\text{pcf}1}/\text{V}$	$E_{\text{paf}1}/\text{V}$	$E_{\text{paf}2}/\text{V}$	$i_{\text{pcf}1}/\mu\text{A}$	$i_{\text{paf}1}/i_{\text{pcf}1}$
0.07	-1.673	-1.572	-1.058	2.130	0.78
0.09	-1.679	-1.569	-1.037	2.412	0.80
0.11	-1.682	-1.569	-1.020	2.662	0.81
0.13	-1.687	-1.565	-1.012	2.871	0.83
0.15	-1.689	-1.559	-1.002	3.078	0.85
0.20	-1.695	-1.554	-0.987	3.513	0.87
0.25	-1.698	-1.552	-0.981	3.861	0.89
0.30	-1.703	-1.546	-0.975	4.209	0.90
0.35	-1.710	-1.542	-0.968	4.498	0.91

The kinetic analyses for electrochemical reaction 8 were also carried out by the same procedure as explained in the  $\text{UO}_2(\text{saloph})\text{DMSO}$  system. The  $\alpha n_B$  value was evaluated to be 0.67 from eq 5, and hence, the  $D_O$  value for  $\text{UO}_2(\text{saloph})\text{DMF}$  in DMF was estimated as  $3.4 \times 10^{-6}$   $\text{cm}^2\cdot\text{s}^{-1}$  by eq 4. The  $\psi$  values are in the range from 0.55 ( $\nu = 0.07$   $\text{V}\cdot\text{s}^{-1}$ ,  $\Delta E_p = 0.101$ ) to 0.17 ( $\nu = 0.35$   $\text{V}\cdot\text{s}^{-1}$ ,  $\Delta E_p = 0.168$ ).<sup>20,21</sup> Therefore, the  $k^0$  value for the electrochemical reaction 8 is estimated as  $2.5 \times 10^{-3}$   $\text{cm}\cdot\text{s}^{-1}$  by using eq 3.

The equation  $\Lambda = 8.7 \times 10^1 k^0/\nu^{1/2}$  is derived from eq 6 for this electrochemical system under  $D_O = D_R$  and  $\alpha = 0.67$  ( $n_B = 1$ ). Hence, the following relationships for a  $k^0$  value are obtained at  $\nu = 0.07$ – $0.35$   $\text{V}\cdot\text{s}^{-1}$ . For a reversible system,  $k^0 > (0.45-1.0) \times 10^{-1}$ , for a quasireversible system,  $(0.45-1.0) \times 10^{-1} > k^0 > (1.4-3.1) \times 10^{-6}$ , and for an irreversible system,  $(1.4-3.1) \times 10^{-6} > k^0$ .

The  $k^0$  value ( $= 2.5 \times 10^{-3}$   $\text{cm}\cdot\text{s}^{-1}$ ) for electrochemical reaction 8 is comparable to that in the quasireversible region.

Therefore, it is concluded that the electrochemical reduction of  $\text{U}^{\text{VI}}\text{O}_2(\text{saloph})\text{DMF}$  in DMF produces the  $[\text{U}^{\text{V}}\text{O}_2(\text{saloph})\text{DMF}]^-$  complex quasireversibly and is accompanied by the structural change of  $[\text{U}^{\text{V}}\text{O}_2(\text{saloph})\text{DMF}]^-$ .

**3.3.  $\text{UO}_2(\text{saloph})\text{L}$  in Mixed Solvents of Dichloromethane and L.** As already mentioned, it was suggested that the successive reaction corresponds to the structural change of  $[\text{U}^{\text{V}}\text{O}_2(\text{saloph})\text{DMF}]^-$ . As the candidates of such

(24) Bard, A. J.; Faulkner, L. R. *Electrochemical Methods Fundamentals and Applications*, 2nd ed.; John Wiley & Sons: New York, 2001. As described at page 473 in this reference, a reaction mechanism in which the sequence involves a chemical reaction of the product after the electron transfer is designated an EC reaction.

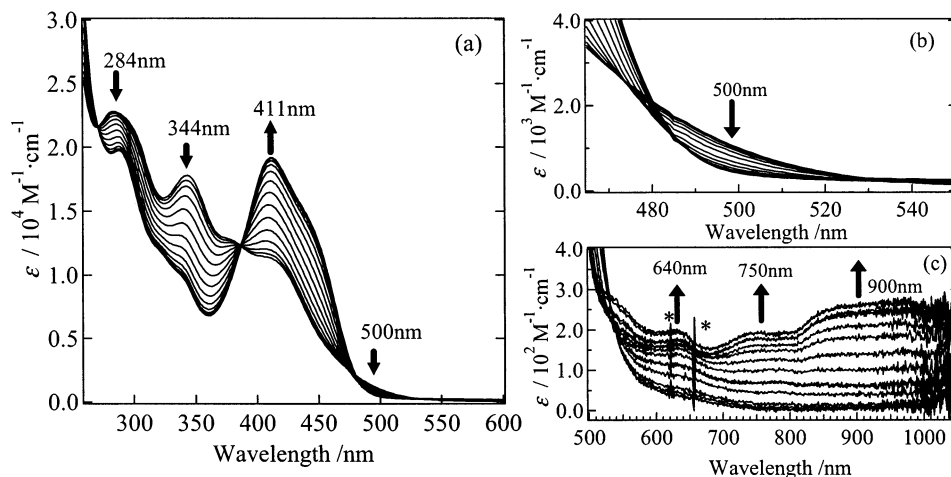


**Figure 7.** Electronic spectra measured at the applied potentials in the range from 0 to  $-1.785$  V for  $\text{UO}_2(\text{saloph})\text{DMF}$  ( $9.33 \times 10^{-4}$  M) in DMF solution containing 0.30 M TBAP. Wavelength range: (a) 260–600, (b) 465–550, and (c) 500–1050 nm. Asterisk indicates noise of equipment.

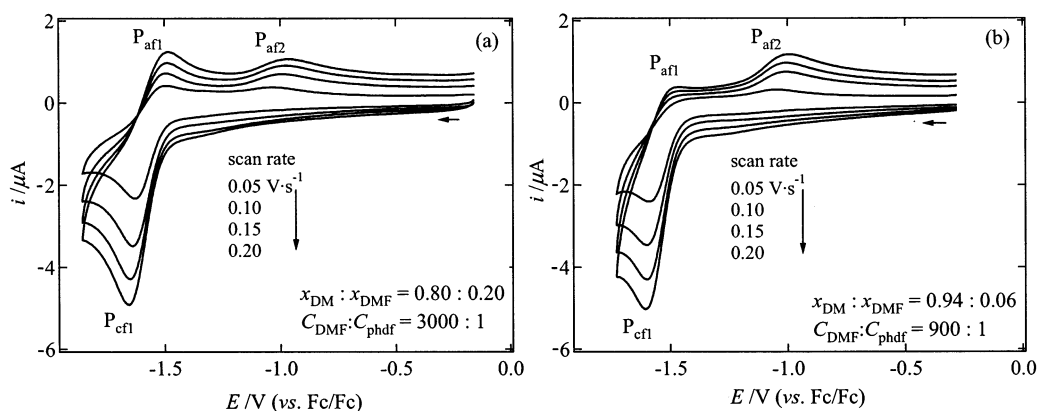


**Figure 8.** Cyclic voltammograms of  $\text{UO}_2(\text{saloph})\text{DMF}$  [(a)  $9.87 \times 10^{-4}$  and (b)  $9.49 \times 10^{-4}$  M] in DM + DMF containing 0.10 M TBAP at different scan rates ( $\nu = 0.05\text{--}0.20$   $\text{V}\cdot\text{s}^{-1}$ ). Initial scan direction: cathodic.

structural changes, the dissociation of coordinated DMF molecule or one part of  $\text{saloph}^{2-}$  ligand from  $\text{U}^{\text{VO}_2^+}$  can be proposed. If the coordinated DMF is dissociated, the current values at  $E_{\text{paf1}}$  and  $E_{\text{paf2}}$  should decrease and increase with decreasing free DMF concentration ( $C_{\text{DMF}}$ ), respectively. If one part of  $\text{saloph}^{2-}$  ligand is dissociated, such current dependences on  $C_{\text{DMF}}$  should not be observed.

The CV measurements of  $\text{UO}_2(\text{saloph})\text{DMF}$  in mixed solvents of dichloromethane (DM) and DMF (DM + DMF) were carried out to examine the current dependence on  $C_{\text{DMF}}$ . The resulting cyclic voltammograms are shown in Figure 8. As expected, the peaks ( $P_{\text{cfl}}$ ,  $P_{\text{af1}}$ , and  $P_{\text{af2}}$ ) are observed at similar potentials to those in Figure 6, and the current values at  $E_{\text{paf1}}$  and  $E_{\text{paf2}}$  decrease and increase with decreasing the ratio of  $C_{\text{DMF}}$  to the concentration of  $\text{UO}_2(\text{saloph})\text{DMF}$  ( $C_{\text{phdf}}$ ), respectively. From these results, it is revealed that the structural change is the dissociation of coordinated DMF from  $[\text{U}^{\text{VO}_2}(\text{saloph})\text{DMF}]^-$ ; that is,  $[\text{U}(\text{V})_{\text{scc}}]$  and  $[\text{U}(\text{VI})_{\text{scc}}]$  are  $[\text{U}^{\text{VO}_2}(\text{saloph})]^-$  and  $\text{U}^{\text{VI}}\text{O}_2(\text{saloph})$ , respectively.

To confirm whether the same phenomenon is observed in the  $\text{UO}_2(\text{saloph})\text{DMSO}$  complex, similar CV experiments were performed for  $\text{UO}_2(\text{saloph})\text{DMSO}$  in mixed solvents of DM and DMSO (DM + DMSO). The results are shown in Figure 9. An uncoupled second oxidation peak ( $P_{\text{as2}}$ ),

which does not appear in the cyclic voltammograms in DMSO (see Figure 2), is observed at ca.  $-1.1$  V ( $E_{\text{pas2}}$ ). The current values at  $E_{\text{pas}}$  and  $E_{\text{pas2}}$  decrease and increase with a decrease in the ratio of the concentration of DMSO ( $C_{\text{DMSO}}$ ) to that of  $\text{UO}_2(\text{saloph})\text{DMSO}$  ( $C_{\text{phds}}$ ), respectively. Furthermore, the  $P_{\text{as2}}$  peak in Figure 9 appears at a similar potential to  $P_{\text{af2}}$  in Figures 6 and 8. Consequently, it is clarified that the electrochemical reduction of  $\text{U}^{\text{VI}}\text{O}_2(\text{saloph})\text{DMSO}$  in DM + DMSO is accompanied by a dissociation of coordinated DMSO from  $[\text{U}^{\text{VO}_2}(\text{saloph})\text{DMSO}]^-$ .

Furthermore, from the cyclic voltammograms swept several times for  $\text{UO}_2(\text{saloph})\text{L}$  in L and DM + L, it was confirmed that the reduction peak coupled with  $P_{\text{as2}}$  or  $P_{\text{af2}}$  is not observed and that the current values at other peaks are almost constant. These suggest that the  $\text{U}^{\text{VI}}\text{O}_2(\text{saloph})$  complex produced at  $E_{\text{pas2}}$  or  $E_{\text{paf2}}$  is quickly recombined by free L molecule.

As a result, the basic reaction mechanism of  $\text{UO}_2(\text{saloph})\text{L}$  in nonaqueous solvents can be concluded to be shown in Scheme 1.

In the case of  $\text{UO}_2(\text{saloph})\text{DMSO}$  in DMSO ( $C_{\text{DMSO}} = 14$  M,  $C_{\text{phds}} = 9.55 \times 10^{-4}$  M) in Figure 2, the equilibrium between **II** and **III** should be shifted to **II** almost completely, because of about 14000 large excess of  $C_{\text{DMSO}}$  to  $C_{\text{phds}}$ . Thus,

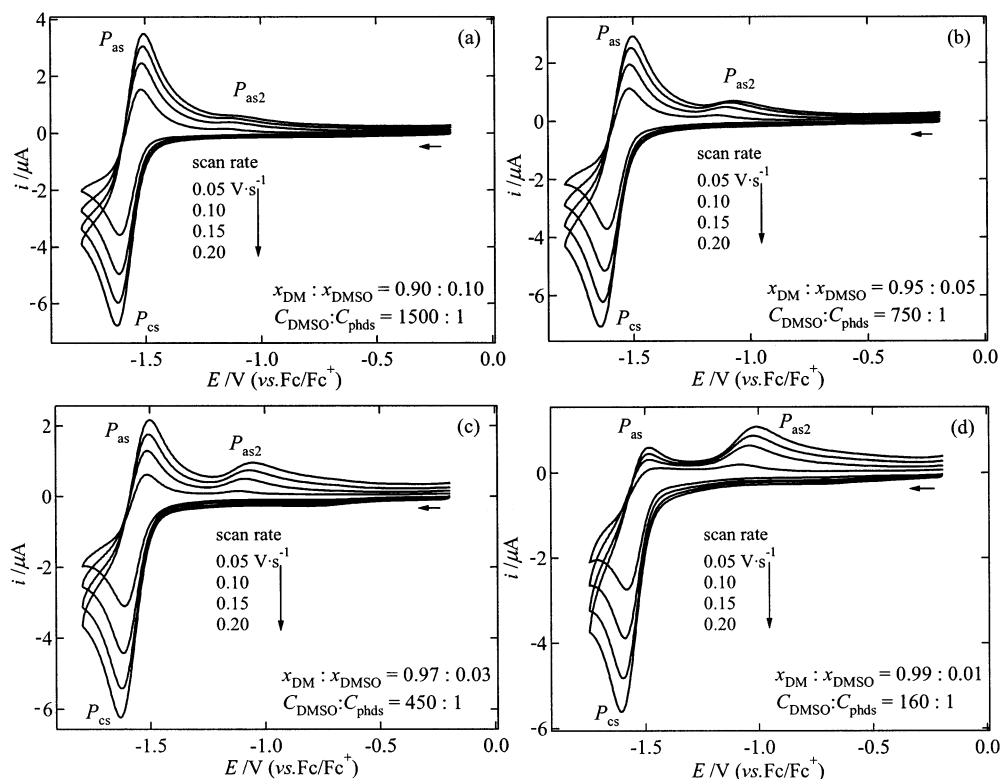
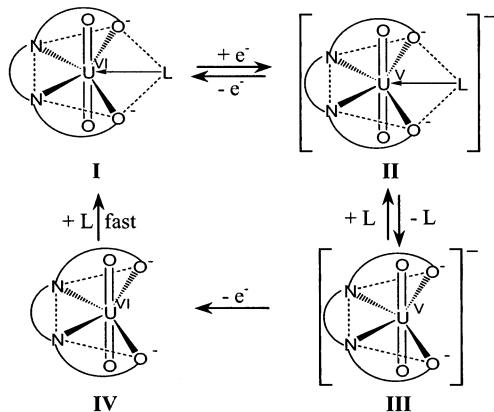


**Figure 9.** Cyclic voltammograms of  $\text{UO}_2(\text{saloph})\text{DMSO}$  [(a)  $1.11 \times 10^{-3}$ , (b)  $1.09 \times 10^{-3}$ , (c)  $1.08 \times 10^{-3}$ , and (d)  $1.14 \times 10^{-3}$  M] in DM + DMSO containing 0.10 M TBAP at different scan rates ( $\nu = 0.05\text{--}0.20$   $\text{V}\cdot\text{s}^{-1}$ ). Initial scan direction: cathodic.

**Scheme 1.** Basic Mechanism of Electrochemical Reactions of  $\text{UO}_2(\text{saloph})\text{L}$  in Nonaqueous Solvents



the only quasireversible electrochemical reaction between **I** and **II** is observed in Figure 2. However, in the case of  $\text{UO}_2(\text{saloph})\text{DMF}$  in DMF ( $C_{\text{DMF}} = 13$  M,  $C_{\text{phdf}} = 8.71 \times 10^{-4}$  M) in Figure 6, species **III** is detected despite about 13000 large excess of  $C_{\text{DMF}}$  to  $C_{\text{phdf}}$ . Such differences suggest that the coordination ability of DMF to  $[\text{U}^{\text{V}}\text{O}_2(\text{saloph})]^-$  is lower than that of DMSO. This should be supported by the following data. We roughly estimated the equilibrium constants ( $K$ ) for  $\text{II} = \text{III} + \text{L}$  in Scheme 1 to be 0.5 M for  $\text{L} = \text{DMSO}$  from the current values at  $P_{\text{cs}}$  and  $P_{\text{as}}$  in Figure 9, and 5 M for  $\text{L} = \text{DMF}$  from those at  $P_{\text{cfl}}$  and  $P_{\text{afl}}$  in Figures 6 and 8.<sup>25</sup> These  $K$  values suggest that the dissociation of DMF in  $[\text{U}^{\text{V}}\text{O}_2(\text{saloph})\text{DMF}]^-$  occurs more easily than that of DMSO in  $[\text{U}^{\text{V}}\text{O}_2(\text{saloph})\text{DMSO}]^-$ . Furthermore, the coordination abilities of  $\text{L}$  to  $[\text{U}^{\text{V}}\text{O}_2(\text{saloph})\text{L}]^-$  are expected

to be lower than those to  $\text{U}^{\text{VI}}\text{O}_2(\text{saloph})\text{L}$ , because the  $\text{L}$  in  $[\text{U}^{\text{V}}\text{O}_2(\text{saloph})\text{L}]^-$  dissociates even in the existence of a large amount of free  $\text{L}$ . To roughly estimate the rate constants for dissociation reactions of  $\text{L}$  in  $[\text{U}^{\text{V}}\text{O}_2(\text{saloph})\text{L}]^-$ , we measured apparent first-order rate constants ( $k_{\text{ex}}$ ,  $\text{s}^{-1}$ ) for exchange reactions of  $\text{L}$  in  $\text{U}^{\text{VI}}\text{O}_2(\text{saloph})\text{L}$  in dichloromethane- $d_2$  by using an NMR line-broadening method. The resulting  $k_{\text{ex}}$  values are  $1.7 \times 10^2$   $\text{s}^{-1}$  for  $\text{L} = \text{DMSO}$  and  $4.6 \times 10^2$   $\text{s}^{-1}$  for  $\text{L} = \text{DMF}$  at 25 °C. It is supposed from these data that the rate constants for dissociation reactions of  $\text{L}$  in  $[\text{U}^{\text{V}}\text{O}_2(\text{saloph})\text{L}]^-$  are more than  $2 \times 10^2$   $\text{s}^{-1}$  at 25 °C.

#### 4. Summary

In the present study, we elucidated the electrochemical properties of  $\text{UO}_2(\text{saloph})\text{L}$  ( $\text{L} = \text{DMSO}$  or  $\text{DMF}$ ) in nonaqueous solvents. The basic electrochemical reaction of  $\text{UO}_2(\text{saloph})\text{L}$  in nonaqueous solvents can be concluded to be a quasireversible system accompanied by  $\text{L}$  dissociation from  $[\text{U}^{\text{V}}\text{O}_2(\text{saloph})\text{L}]^-$ . It is reconfirmed that the uranyl complexes with tetradentate ligands in the uranyl equatorial plane can produce more stable  $\text{U}(\text{V})$  complexes than those with uni- or bidentate ligands.<sup>5–7</sup> In the present systems, it is

(25) Current values at reduction and oxidation peaks of a redox couple ( $i_{\text{pc1}}$  and  $i_{\text{pa1}}$ , respectively) in cyclic voltammograms should be proportional to initial concentrations of oxidant and reductant, respectively. Therefore, it is possible to roughly evaluate the equilibrium constant ( $K$ ) for the  $[\text{U}^{\text{V}}\text{O}_2(\text{saloph})\text{L}]^-$  (**II**) =  $[\text{U}^{\text{V}}\text{O}_2(\text{saloph})]^-$  (**III**) +  $\text{L}$  in Scheme 1 by using  $K = \frac{[\text{III}][\text{L}]}{[\text{II}]} = \frac{C_0 \times (1 - i_{\text{pa1}}/i_{\text{pc1}}) \times C_{\text{L}}}{\{C_0 \times (i_{\text{pa1}}/i_{\text{pc1}})\}}$ , where  $C_0 = [\text{I}] = [\text{III}] + [\text{II}] = C_0 \times (i_{\text{pa1}}/i_{\text{pc1}})$ ,  $[\text{III}] = C_0 \times (1 - i_{\text{pa1}}/i_{\text{pc1}})$ , and  $C_{\text{L}} = [\text{L}]$ .

clarified that the coordination abilities of L to  $[\text{U}^{\text{V}}\text{O}_2(\text{saloph})]^-$  are lower than those to  $\text{U}^{\text{VI}}\text{O}_2(\text{saloph})$  and that this ability of DMF to  $[\text{U}^{\text{V}}\text{O}_2(\text{saloph})]^-$  is lower than that of DMSO.

Furthermore, we obtained the electronic spectrum of pure  $[\text{U}^{\text{V}}\text{O}_2(\text{saloph})\text{DMSO}]^-$  complex in DMSO. It is revealed that the disappearance of the absorption band at around 500 nm and the appearance of those at around 750 and 900 nm are characteristics of the  $[\text{U}^{\text{V}}\text{O}_2(\text{saloph})\text{DMSO}]^-$  complex in DMSO.

**Acknowledgment.** We would like to thank Prof. Kunio Shimizu and Dr. Takeshi Hashimoto and his laboratory members (Sophia University) for the precious opinions about the OTTLE cell, Dr. Tsuyoshi Arai (Institute of Research and Innovation) for the elemental analysis, and Dr. Masayuki Harada (Tokyo Institute of Technology) for technical assistance.

IC0260926